Preparation and Characterization of Poly(vinyl Alcohol)-Based Magnetic Nanocomposites. 1. Thermal and Mechanical Properties

DANIEL LÓPEZ,[1] IONE CENDOYA,[1] F. TORRES,[2] JAVIER TEJADA,[2] CARMEN MIJANGOS[1]

[1] Instituto de Ciencia y Tecnología de Polímeros, C.S.I.C., Juan de la Cierva 3, E-28006 Madrid, Spain

[2] Dept. Fisica Fonamental, Facultat de Fisica, Universitat de Barcelona, Avinguda Diagonal 647, E-08028 Barcelona, Spain

Received 27 November 2000; accepted 15 January 2001

ABSTRACT: $CoFe_2O_4$ magnetic nanoparticles were prepared by in situ precipitation and oxidation of Co^{2+} and Fe^{2+} within a sulfonated polystyrene resin. The nanometric particles were characterized by X-ray diffraction. A ferrofluid was prepared from the $CoFe_2O_4$ mineralized polymer resin and water. Poly(vinyl alcohol) (PVA)-based nanocomposite materials were obtained by mixing different amounts of ferrofluid (compositions ranging within 0–51 wt % of mineralized resin) with an aqueous solution of the polymer. The PVA composite materials were characterized by TGA, DSC, and stress–strain testing. The thermal and mechanical properties of PVA change with filler content, exhibiting an initial increase in these properties due to polymer–filler interactions. After a maximum value, at about 15 wt % of mineralized resin, the mechanical properties decrease probably due to particle aggregation which causes phase separation. The results obtained show that the nanoparticles are dispersed in the amorphous regions of the polymer, the crystalline zones remaining unaltered up to compositions as high as 30 wt %. © 2001 John Wiley & Sons, Inc. J Appl Polym Sci 82: 3215–3222, 2001

Key words: poly(vinyl alcohol); $CoFe_2O_4$; nanocomposite; thermal properties; mechanical properties

INTRODUCTION

Recently, the design and synthesis of materials with nanometer dimensions have been subject of intense research.[1] Materials with nanoparticles display novel electronic, optical, magnetic, and chemical properties, owing to their exceptionally small dimensions.[2] Whereas numerous studies have been devoted to the synthesis of nanometer-size compound semiconductors, relatively little work exists on magnetic materials of similar dimensions.[3–6] Potential applications for the latter include electronic circuitry, sensors, switches, generators, magnetic refrigeration, information storage, and electrical transformers.[7–12]

The crucial point in obtaining nanosize materials is to prevent particles from aggregating.[1,13] By the use of a polymer matrix in the form of a synthetic ion-exchange resin, it is possible to stabilize, isolate, and characterize a mesoscopic form of $CoFe_2O_4$. The formation of these materials can be highly regulated; can show typical structural

Correspondence to: D. López (daniel@ictp.csic.es).

Contract grant sponsor: European Union; Contract grant number: BRST-CT98-5267; Contract grant sponsor: CICYT; Contract grant number: MAT99-1179.

Journal of Applied Polymer Science, Vol. 82, 3215–3222 (2001)

characteristics on the nanometer as well as on the micrometer scale; and can be controlled by the type of polymeric matrix, which acts as a spatially restricted microenvironment and molecular template for inorganic mineralisation.[14–16]

There are basically two different approaches to the formation of mineral–polymer composites.[17,18] The most obvious is the incorporation of preformed inorganic particles into the polymer by grinding and mixing. An alternative is the in situ synthesis of nanoparticles within the polymer matrix. Both methods present different disadvantages. In the first method, the filler particles are not distributed homogeneously in the polymer matrix. Instead of individual particles, aggregates are present, and their size distribution cannot be controlled. In the second method, the composite materials, which are generally obtained in a particulate or gel form, do not exhibit good mechanical properties (compactness, toughness, stiffness) and are not easy to process from a practical point of view.

By contrast, poly(vinyl alcohol) is a polymer that has been studied intensively because of its good film forming and physical properties, high hydrophilicity, processability, biocompatibility and good chemical resistance.[19–21] These properties have led to its broad industrial use, in such areas as fibers manufacture,[22] membranes,[23] textile sizing and finishing,[24] adhesives,[25] and coatings and paints.[26] Furthermore, PVA properties can be improved or modified depending on the polymerization conditions of the parent poly(vinyl acetate) as well as by the hydrolysis conditions, drying, grinding, or chemical modification of the polymer.[20,21]

The present article deals with the preparation and with the thermal and mechanical characterization of a new type of nanocomposite magnetic material, and is part of a more general study of the preparation of composite materials with nano free-rotor magnets.[27,28] We combine the two methods of material preparation mentioned above as a means to avoid the main disadvantages. In a first step, we prepare the magnetic nanoparticles by in-situ precipitation within an ion-exchange sulfonated polystyrene resin in order to prevent particle aggregation. In the second step, we disperse the ferrofluid prepared from this composite in a PVA matrix to improve the processability and the properties of the nanocomposite material.

EXPERIMENTAL

Materials

Crosslinked polystyrene sulfonic acid sodium salt, with an exchange capacity of 4.3 mEq/g, was purchased from Scientific Polymer Products. Cobaltous chloride hexahydrate and ferrous chloride tetrahydrate were purchased from Fluka and were used without further purification. Poly(vinyl alcohol), > 99% hydrolyzed, with a weight average molecular weight of 94,000 g/mol and a tacticity of syndio = 17.2%, hetero = 54.1%, and iso = 28.7%, was purchased from Aldrich and was used without further purification.

Mineralization of the Polymer Resin

The sulfonated polystyrene resin was exchanged with Fe(II) and Co(II) (molar ratio 2 : 1) from an aqueous solution of the respective chlorides, followed by thorough washings to remove excess physisorbed ions. The resin was then exposed to a 0.5*M* aqueous solution of sodium hydroxide at 60°C, which causes precipitation of the corresponding hydroxide and the conversion to oxide. After stirring for several hours, the resin was thoroughly washed with distilled water to neutral pH and dried. The ion-exchange capability of the resin remained intact[1] after the above treatments; resin containing more oxide could be prepared by repeating the above-mentioned procedure six times. The mineralized resin was then dried in vacuum at 100°C until a constant weight was reached.

Wide-angle X-ray diffraction (WAXD) patterns from the mineralized resin were obtained at room temperature, using a Philips Geiger X-ray diffractometer operating in a 2θ range between 2° and 72° at a rate of 1°/min, using Ni-filtered CuKα radiation.

Ferrofluid Preparation

Stable water ferrofluid was prepared in the following way. The mineralized polymer resin was roll-milled for 4 days. The fine powder obtained was then wet milled for 24 h by adding the appropriate amount of deionized water. The liquid was separated from the shot and then centrifuged at 6000 rpm, 4 times, at 30-min intervals. The liquid was then concentrated in an Amicon 8050 ultrafiltration cell using a YM30 membrane under N_2 gas.

Composite Material Preparation

Poly(vinyl) alcohol-based composite materials were obtained by mixing the appropriate amount of ferrofluid with an aqueous solution of PVA. When homogenization was obtained, polymer films were prepared by pouring the solution into glass plates and allowing the water to evaporate at room temperature. The films were dried under vacuum at 50°C for 24 h. Samples with a mineralized sulfonated polystyrene content ranging from 0 to 51% (w/w) were prepared.

Composite Material Characterization

The thermal stability of the composite materials was evaluated by thermogravimetric analysis (TGA) performed on a Perkin–Elmer TGA-7, using a nitrogen stream as purge gas, at a heating rate of 10°C/min with the range of 40–800°C.

The differential scanning calorimetry (DSC) curves were obtained with a Perkin–Elmer DSC-7 system, in aluminium pans at heating or cooling rates of 10°C/min, under nitrogen. The glass-transition temperature (T_g) values were taken from the midpoint of the transitions, and the T_m values from the maximum of the melting peak, both in the second scan.

The mechanical properties were studied from the stress–strain curves obtained in a MTS Synergie 200 testing machine. Measurements were carried out using a 0.1 KN load cell, with a testing speed of 5 mm/min, at room temperature, employing dumbbell-shaped test samples.

RESULTS AND DISCUSSION

From the peak positions and the relative intensities of the WAXD patterns, it was possible to identify the oxide phase of the mineralized sulfonated polystyrene as the inverse spinel $CoFe_2O_4$ (Fig. 1). The average diameter of the $CoFe_2O_4$ particles was 20 nm, as determined from the widths of the peaks using the following equation[29]:

$$\langle d \rangle = \frac{1.38762}{\mathrm{FWHH}\,\frac{\pi}{180}\cos\left(2\theta_{\mathrm{peak}}\,\frac{\pi}{360}\right)}$$

where $\langle d \rangle$ is the average particle diameter, FWHH is the full width at half-height of the main peak and $2\theta_{\mathrm{peak}}$ its position.

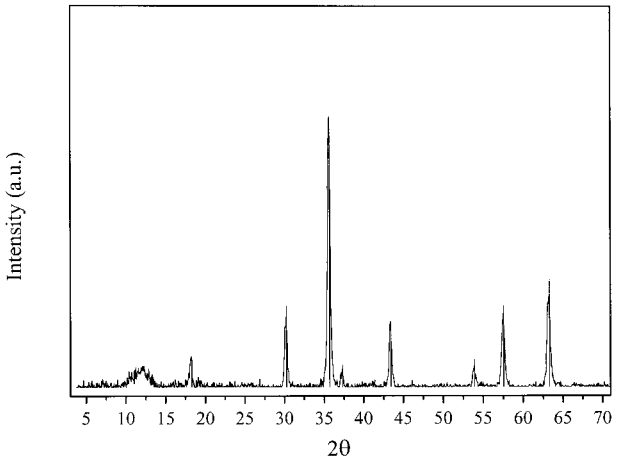

Figure 1 X-ray diffraction pattern of the mineralized polymer resin. Vertical lines correspond to the theoretical positions and relative intensities of the inverse spinel $CoFe_2O_4$ diffraction peaks.

The magnetic characterization of the mineralized sulfonated polystyrene shows the existence of magnetic oxide nanoparticles with a very narrow size distribution and an average value between 6 to 10 nm.[27] These values are in all cases lower than those deduced from WAXD, suggesting that the magnetic core of the particles corresponds to only one fraction of the total crystallographic volume. At room temperature, the mineralized polymer shows coercive fields values between 500 and 900 Oe and saturation magnetization of about 500 emu/cm^3.[27]

Characterization of the mineralized sulfonated polystyrene by TGA reveals an oxide content of approximately 12.4 wt %. The ferrofluid composition was determined by TGA to be 15.1 wt % in solids and 1.9 wt % in oxide. The particle size of the dispersed solids was 8 nm on average, as determined by transmission electron microscopy (TEM) and by magnetic measurements.[27]

Thermal Stability

The thermal stability of the PVA and the composite materials was studied by TGA. In Figure 2, the TGA thermograms of PVA and five samples with compositions ranging from 0 to 51 wt % are compared. Three degradation steps can be observed. The first weight loss process, which is associated with the loss of absorbed moisture and/or with the evaporation of trapped solvent,[30] is independent of the composition for all the samples. Only a slight difference is observed for the 51 wt % sam-

ple where the loss of moisture begins at lower temperatures. Nevertheless, all the samples present the same degree of absorbed water, as can be inferred from the thermograms, showing that the preparation conditions for all the samples are similar.

The second weight loss process corresponds to the degradation of the PVA by a dehydration reaction on the polymer chain.[30] Two effects can be observed: (1) as expected, the weight loss percentage depends on the composite material composition; and (2) the position of the associated decomposition temperature is shifted to higher temperatures with increasing filler content, as can be seen in Figure 3. The decomposition temperature of PVA increases from about 250 to 300°C. The reason for the increment in polymer stability is not well understood, but it may be related to the restriction in polymer chain mobility and to the reduction of diffusivity of attacking agents within the polymer matrix, both attributable to polymer–filler interactions.[31]

The increment of the decomposition temperature as a function of the filler content reaches a maximum value at about 30 wt %, and then the decomposition temperature experiments a slight reduction (Fig. 3). The decrease of thermal stability may be explained by (1) the formation of filler aggregates or agglomerates leading to a certain phase separation into a polymer-rich phase and a filler-rich phase, or (2) the inclusion of the excess of filler in the crystalline regions of the polymer with the consequent decrease of the crystallinity. The results obtained by DSC support the first explanation.

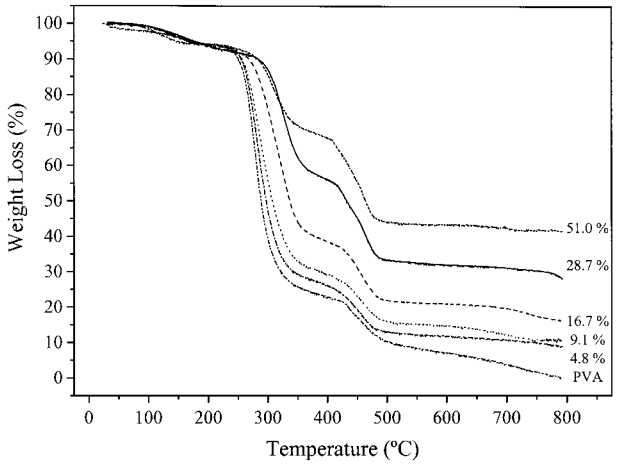

Figure 2 Weight loss as a function of temperature for PVA and the different composite materials. Filler content (wt %) of the composites are indicated.

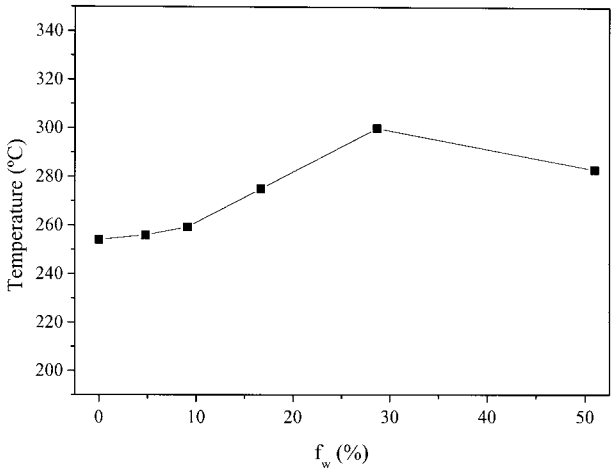

Figure 3 Initial temperature of decomposition of a series of composite materials as a function of filler content, f_w, (wt %).

In the third weight loss process, the polyene residues are further degraded at approximately 450°C[31] to yield carbon and hydrocarbons. The degradation temperature corresponding to this weight loss process is independent of the filler content. This result is in agreement with the almost absence of interactions between the residual polyene and the filler.

Another interesting point is the fact that the residual weight at 800°C is greater than the expected value for all the samples with compositions smaller than ~ 30 wt %. The pure mineralized resin presents a residual weight of 54.9% at 800°C. Considering that the PVA decomposes completely within the composite material, as occurs for the pure polymer, the residual weight would be smaller than the measured value. To verify this point, we measured the thermal degradation of sulfonated polystyrene–poly(vinyl alcohol) blends. The results obtained show that the sulfonated polystyrene produces an additional stabilization of the final degradation products of PVA, which do not decompose completely at 800°C for compositions of the blends smaller than 50%. For example, for a sulfonated polystyrene–PVA blend of 28–72 wt %, the residual weight obtained at 800°C was 18% and, considering the complete degradation of PVA, the residual weight should be ~ 11.9%.

Thermal Behavior

Glass-Transition Temperature, T_g

Study of the thermal transitions of PVA and the composite samples was performed by DSC mea-

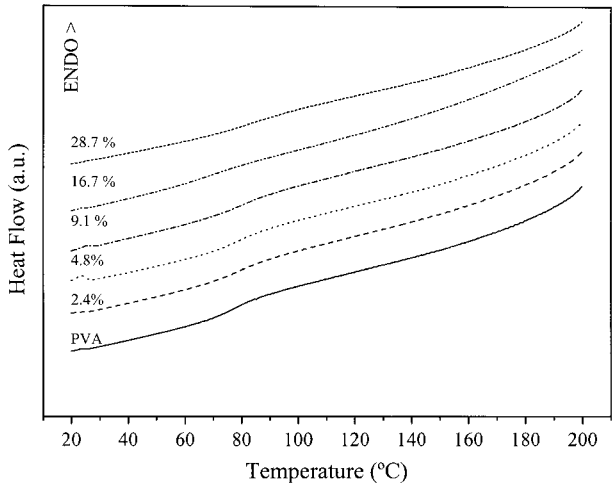

Figure 4 DSC curves showing the glass transition of PVA and five nanocomposite samples. Filler contents (wt %) are indicated.

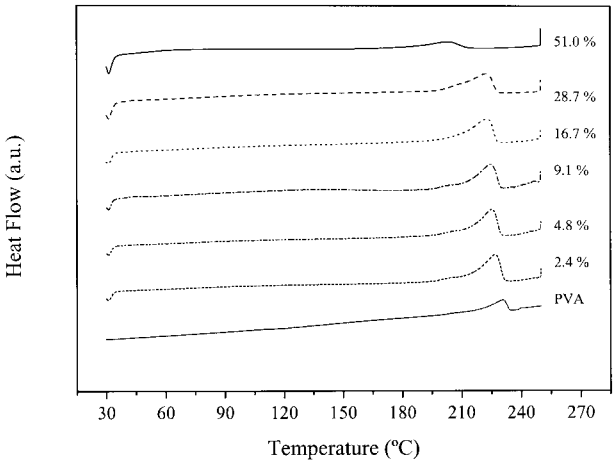

Figure 6 DSC curves showing the melting peaks of PVA and five nanocomposite samples. Filler contents (wt %) are indicated.

surements. The DSC curves obtained for various samples are represented in Figure 4. In all cases, only one transition corresponding to the glass transition of PVA was detected in the interval of temperatures studied. The glass transition temperature corresponding to the pure sulfonated polystyrene resin at 180°C was not observed in any case. The T_g values obtained for PVA from these DSC curves are plotted against the filler content in Figure 5. An increase of the glass transition temperature is seen up to conversions of $\sim$ 30 wt %. For higher filler contents, a deviation from the expected behavior is observed, and the

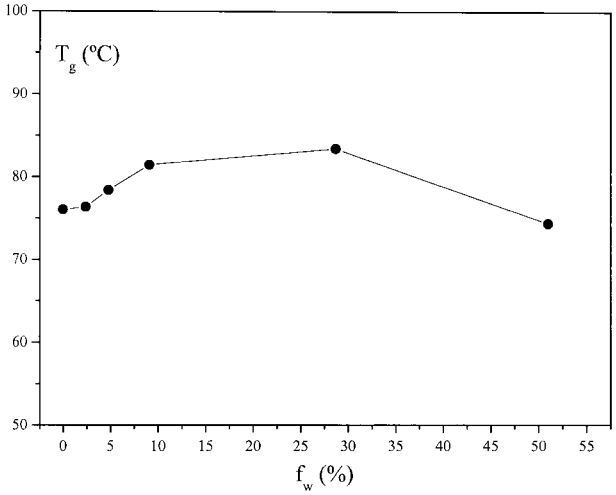

Figure 5 Dependence of the glass-transition temperature on filler content, f_w (wt %). Solid line is an optical guide.

T_g values decrease with composition. As explained earlier, in the description of thermal stability, physical interactions between PVA and the filler reduce the polymer chain mobility and produce an increase in the glass-transition temperature.[31] For higher filler contents, a phase separation may occur, as indicated above, leading to filler agglomerates and a polymer-rich phase with reduced polymer–filler.

The glass-transition temperature corresponding to the mineralized sulfonated polystyrene can be observed in Figure 6, where the temperature range studied was expanded. The T_g values of the $CoFe_2O_4$-loaded resin shift 20°C with respect to the pure resin, but do not depend on the composition for the different samples of the PVA-based composite materials. The increment of T_g may be explained by the interactions between the sulfonic groups of polystyrene and the hydroxyl groups at the surface of the cobalt iron oxide nanoparticles, the latter reducing the mobility of polystyrene.

Melting Temperature, T_m

Other DSC studies (Fig. 6) show the melting endotherm of PVA crystallites. The PVA sample used in this study is essentially atactic but has a degree of crystallinity of about 40%. Furthermore, PVA is a semicrystalline polymer in which high physical interactions between polymer chains exist, due to hydrogen bonding between hydroxyl groups. The introduction of nanosized fillers can affect both crystallinity and the physical network,

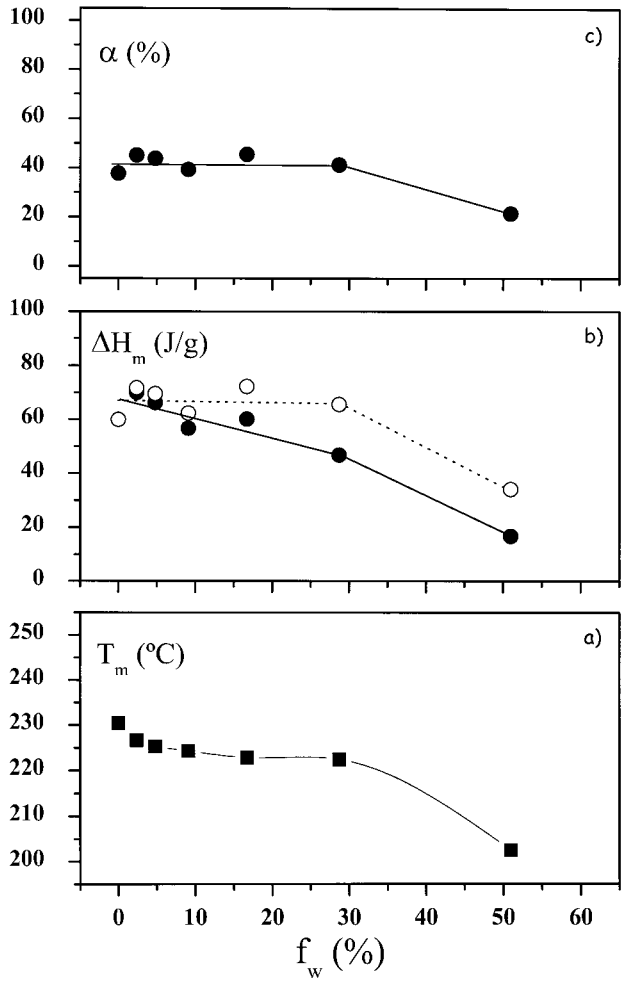

Figure 7 Variation of (a) melting temperature; T_m, (b) enthalpy of melting, ΔH_m, (●) as measured; (○) refers to the polymer content in the composite material; and (c) degree of crystallinity, α, as a function of filler content f_w (wt %).

causing the variations in both the T_g values as seen above, and in the melting enthalpy and temperature.

In Figure 7(a), the variation of the melting temperature with the filler content is shown. T_m diminishes progressively from 230 to 225°C for filler contents ranging within 0–30 wt %. Subsequently, the variation is more pronounced and the T_m drops by 20°C between a filler content of 30 and 50 wt %. This decrease in the melting temperature might be related to a decrease in the crystallinity of the sample, and perfection of the crystal structure due to the inclusion of the filler in the crystalline regions of the PVA, or to a lower polymer content as the filler content increases. To check whether the filler is located in the crystalline zones of the composite material, we have studied the dependence of the melting enthalpy and the degree of crystallinity on the filler content. Figure 7(b) shows the variation of the melting enthalpy as a function of composition as measured by DSC. Apparently, there are two different slopes: the value of the melting enthalpy decreases gradually up to a composition of ~ 30 wt % and then is more pronounced up to 50 wt %. However, if one considers the real amount of PVA in the samples, the corrected values of the melting enthalpy (dotted line) show that there is no variation on this magnitude for samples with filler contents of < 30 wt %. This fact can be better observed in Figure 7(c), which shows the variation of the degree of crystallinity, α, with composition. The value of α remains constant up to sample compositions of 30 wt %; the crystallinity then decreases with the filler content. All the results indicate that, for sample compositions smaller than 30 wt %, the nanosized particles are distributed in the amorphous regions of the polymer, since the crystalline parts remain unchanged with respect to the initial PVA. For sample compositions of > 30 wt %, the initial order in the system is broken as a consequence of the formation of filler aggregates.

Mechanical Properties

The mechanical properties of PVA and the composite materials were evaluated from stress–strain curves. They were tested for tensile strength, Young's Modulus and elongation at break. As an example, the stress–strain curves for PVA, and two samples of different compositions are plotted in Figure 8, where the effect of the filler in the mechanical properties can be observed.

Figure 9(a) and 9(b) present the elongation at break and Young's modulus, respectively, as a function of the filler content. The elongation at break decreases sharply as the filler composition increases (by more than 50% from a filler content of 0–2.4%), leading to very short elongations with respect to those of PVA. By contrast, the Young's modulus increases with increasing filler content, reaching a maximum value at ~ 17 wt %. For higher compositions, the Young's modulus decreases.

The decrease in elongation at break arises from the fact that the actual elongation experienced by the polymer matrix in the composite is much greater than the measured elongation of the spec-

imen[32]; although the specimen is part filler and part matrix, all the elongation comes from the polymer if the filler is rigid. The sharp decrease in elongation at break, even at smaller filler contents, is an indication of the good adhesion between the phases.[33] In the case of poor adhesion between the phases the elongation at break would be expected to decrease more gradually than observed.

Rigid particulate fillers increase the modulus of polymer matrices when there is good adhesion between the two components.[34] The increment in the elastic modulus obtained for our systems can be accounted for by the interactions involving the PVA and the filler nanoparticles. Nevertheless, for conversions of $>$ 15 wt %, the elastic modulus diminishes with increasing filler content. This phenomenon can be explained if we consider the agglomeration of the filler particles.[35,36] Indeed, the aggregation of the filler nanoparticles produces a decrease of the surface area of the filler and consequently a smaller polymer–filler interface. Clearly, the reduction of the polymer–filler interface diminishes the interactions and, as a consequence, the elastic modulus of the composite.

Parallel studies on the dynamic[28] and magnetic properties[27] of the same nanostructured composite materials support the results presented in this article. In particular, the coercitivity of the samples increases with increasing filler content, clearly indicating the aggregation of the magnetic particles. Furthermore, the results are consistent with the fact that the filler aggregation takes place through weak interactions that should be broken by the application of a magnetic field treatment.[27]

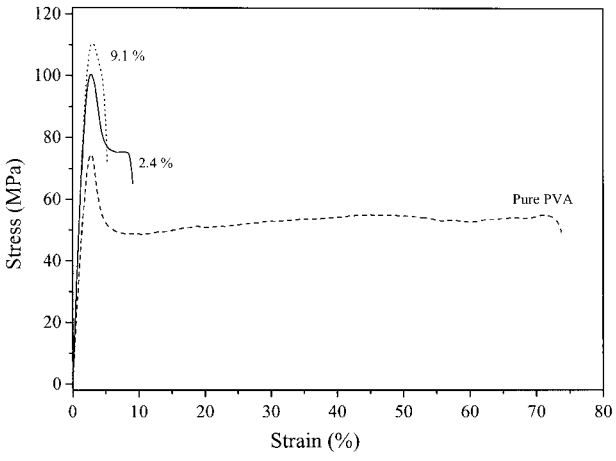

Figure 8 Stress-strain curves for PVA and two composite materials. Filler content: 2.4 and 9.1 (wt %).

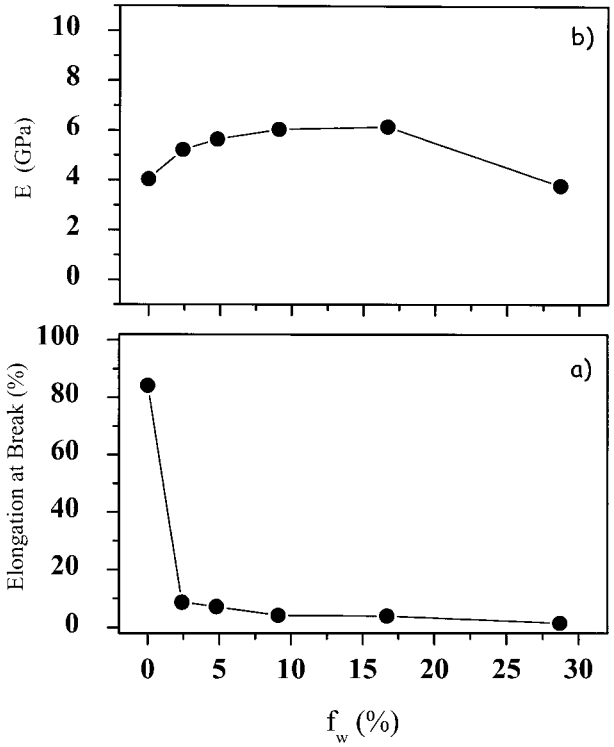

Figure 9 (a) Elongation at break. (b) Young's modulus for PVA and a series of composite materials as a function of filler content, f_w, (wt %).

CONCLUSIONS

The objective of this study was to prepare a new magnetically-soft free-rotor nanostructured polymer-based material with optimal thermal and mechanical properties for sensor and transformer applications. Our results show that the method of preparation developed here allows one to avoid the main disadvantages mentioned in the introduction. In particular, the aggregation of the magnetic particles can be avoided for moderately high filler contents. By contrast, the processability and the thermal and mechanical properties of the material are improved.

REFERENCES

1. Ziolo, R. F.; Giannelis, E. P.; Weinstein, B. A.; O'Horo, M. P.; Ganguly, B. N.; Mehrotra, V.; Russell, M. W.; Huffman, D. R. Science 1992, 257, 219.

2. Brus, L. E., et al. J Mater Res 1989, 4, 704.
3. Okata, H., et al. Chem Mater 1990, 2, 89.
4. Mann, S.; Hannington, J. P. J Colloid Interface Sci 1988, 122, 326.
5. Zhao, X. K.; Herve, P. J.; Fendler, J. H. J Phys Chem 1989, 93, 908.
6. Papaefthymiou, V., et al. J Appl Phys 1990, 67, 4487.
7. Gunther, L. Phys World 1990, 3, 28.
8. Audran, R. G. L.; Huguenard, A. P. U.S. Patent 1981, 4:302:523.
9. Ziolo, R. F. U.S. Patent 1984, 4:474:866.
10. Nixon, L.; Koval, C. A.; Noble, R. D.; Slaff, G. S. Chem Mater 1992, 4, 117; Marchessault, R. H.; Ricard, S.; Rious, P. Carbihydr Res 1992, 224, 133.
11. McMichael, R. D.; Shull, R. D.; Swartzendruber, L. J.; Bennett, L. H.; Watson, R. E. J Magn Magn Mater 1992, 111, 29.
12. Anton, J., et al. J Magn Magn Mater 1990, 85, 219.
13. Breulmann, M.; Cölfen, H.; Hentze, H.-P.; Antonietti, M.; Walsh, D.; Mann, S. Adv Mater 1998, 10, 237.
14. Mann, S.; Webb, J.; Williams, R. J. P., Eds. Biomineralization: Chemical and Biochemical Perspectives. VCH: Weinheim, 1989.
15. Heuer, A. H.; Fink, D. J.; Laraia, V. J.; Arias, J. L.; Calvert, P. D.; Kendall, K.; Messing, G. L.; Blackwell, J.; Rieke, P. C.; Thompson, D. H.; Wheeler, A. P.; Veis, A.; Caplan, A. J. Science 1992, 255, 1098.
16. Mann, S.; Ozin, G. A. Nature 1996, 382, 313.
17. Beecroft, L. L.; Ober, C. K. Chem Mater 1997, 9, 1302.
18. Zrínyi, M. TRIP 1997, 5, 280.
19. Huang, R. Y. M.; Rhim, J. W. Polym Int 1993, 30, 129.
20. Giménez, V.; Mantecón, A.; Cádiz, V. J. Polym Sci Polym Chem Ed 1996, 34, 925.
21. Krumova, M.; López, D.; Benavente, R.; Mijangos, C.; Pereña, J. M. Polymer 2000, 41, 9265.
22. Sone, T.; Ito, N. Sen'i Gakkaishi 1988, 44, 84.
23. Kuwahara, N.; Kaneko, M.; Kubo, K. Makromol Chem 1967, 110, 294.
24. Ibrahim, N. A.; Trauter, J. Melliand Textilber 1990, 71, 199.
25. Levine, M.; Ilkka, G.; Weis, P. J Polym Sci B 1964, 2, 915.
26. Chiang, W.; Min Hu, C. J Appl Polym Sci 1985, 30, 4045.
27. Cendoya, I.; López, D.; Mijangos, C.; Julià, A.; Torres, F.; Tejada, J. Appl Phys Lett (to appear).
28. Cendoya, I.; López, D.; Alegría, A.; Mijangos, C. J Polym Sci Part B Polym Phys 2001, 39, 1968.
29. Cornell, R. M.; Schwertmann, U. The Iron Oxide; VCH: Weinheim, 1995, p 82.
30. Finch, C. A., Ed. Polyvinyl Alcohol Properties and Applications; Wiley: Chichester, 1973, p 167.
31. Sivarani, S.; Singh, R. P. Adv Polym Sci 1991, 101, 169.
32. Nielsen, L. E. J Appl Polym Sci 1966, 10, 97.
33. Nielsen, L. E., Ed. Mechanical Properties of Polymers and Composites; Marcel Dekker: New York, 1974.
34. Nederveen, C. J.; Bree, H. W. U.S. Dept. of Commerce Rept, AD 655634, 1967.
35. Lewis, T. B.; Nielsen, L. E. J Appl Polym Sci 1970, 14, 1449.
36. Flocke, H. A. Kaut Gummi Kunstst 1965, 18, 717.